

Vortex states of the E_u model for Sr_2RuO_4

Takafumi Kita

Division of Physics, Hokkaido University, Sapporo 060-0810, Japan

(December 3, 2017)

Based on the Ginzburg-Landau functional of E_u symmetry presented by Agterberg, vortex states of Sr_2RuO_4 are studied in detail over $H_{c1} \lesssim H \leq H_{c2}$ by using the Landau-level expansion method. For the field in the basal plane, it is found that (i) the second superconducting transition should be present irrespective of the field direction; (ii) below this transition, a characteristic double-peak structure may develop in the magnetic-field distribution; (iii) a third transition may occur between two different vortex states. It is also found that, when the field is along the c axis, the square vortex lattice may deform through a second-order transition into a rectangular one as the field is lowered from H_{c2} . These predictions will be helpful in establishing the E_u model for Sr_2RuO_4 .

Active studies have been performed on superconducting Sr_2RuO_4 [1] where another unconventional pairing may be realized [2]. A possible candidate for its symmetry is the E_u model with two-fold degeneracy [3], as indicated by various experiments [4–10]. However, further experiments seem being required before establishing its validity for Sr_2RuO_4 . In this respect, the vortex states may provide clear and indisputable tests for the p -wave hypothesis. The present paper provides a detailed theoretical description of them which will be helpful towards that purpose. Clarifying the basic features of the two-component model, which has not been performed completely, will also be useful for the experiments of UPt_3 .

The vortex states of the E_u model for Sr_2RuO_4 have been studied theoretically in a series of papers by Agterberg *et al.* [11–13]. Based on the two-component Ginzburg-Landau (GL) functional and following essentially Abrikosov's method [14] which is effective near the upper (H_{c2}) and lower (H_{c1}) critical fields, they have provided several important predictions. Especially noteworthy among them are: existence of the second transition for $\mathbf{H} \perp \mathbf{c}$ similar to that observed in UPt_3 [15,16]; several orbital-dependent phenomena helpful in identifying which band is mainly relevant; stabilization of the square vortex lattice for $\mathbf{H} \parallel \mathbf{c}$. An observation of the square lattice has been reported by Riseman *et al.* [17].

With these results, this paper focuses on the following: (i) The properties of the intermediate fields, in particular those below the second transition for $\mathbf{H} \perp \mathbf{c}$, remain to be clarified. We will treat the whole range $H_{c1} \leq H \leq H_{c2}$ in a unified way, describe possible changes of experimentally detectable properties as a function of the field strength, and draw characteristic features in low fields. (ii) Considered have been the cases where the field is along the high-symmetry axes. It is still not clear whether or not the second transition for $\mathbf{H} \perp \mathbf{c}$ persists for arbitrary field directions in the ab plane, because the term $|\eta_1|^2|\eta_2|^2$ in the GL functional [see Eq. (1) below] generally causes the first- and third-order mixing. We will study those general cases to establish the existence of the second transi-

sition. (iii) Agterberg introduced several assumptions in the parameters used to minimize the free energy. We will perform the minimization without such assumptions.

The goals (i)-(iii) may seem rather formidable, but they can be achieved with the Landau-level expansion method [18]. When applied to the s -wave pairing, it successfully reproduced the properties of the whole region $H_{c1} \lesssim H \leq H_{c2}$ quite efficiently for an arbitrary κ . Compared with the direct minimization procedure in real space [19], the method has a couple of advantages that (i) it is far more efficient and (ii) one can enumerate possible second-order transitions rather easily, hence enabling us to establish the phase diagram of various multi-order-parameter systems. This is the first time where it is applied to an multi-order-parameter system so that this paper also has some methodological importance.

The GL free-energy density adopted by Agterberg is given by [11]

$$f = -|\boldsymbol{\eta}|^2 + \frac{1}{2}|\boldsymbol{\eta}|^4 + \frac{\gamma}{2}(\boldsymbol{\eta} \times \boldsymbol{\eta}^*)^2 + (3\gamma - 1)|\eta_1|^2|\eta_2|^2 - \boldsymbol{\eta}^\dagger \begin{bmatrix} D_x^2 + \gamma D_y^2 + \kappa_5 D_z^2 & \gamma(D_x D_y + D_y D_x) \\ \gamma(D_x D_y + D_y D_x) & D_y^2 + \gamma D_x^2 + \kappa_5 D_z^2 \end{bmatrix} \boldsymbol{\eta} + h^2, \quad (1)$$

where the same notations are used here. This simplified free energy has the advantage that there are only two parameters in it whose values can be extracted from experiments, i.e. $\kappa_1 \equiv H_{c2}/\sqrt{2}H_c$ and $\nu \equiv \frac{1-3\gamma}{1+\gamma}$, the latter being related to the H_{c2} anisotropy in the ab plane as $H_{c2}(\mathbf{a})/H_{c2}(\mathbf{a} + \mathbf{b}) = \frac{1-\nu}{1+\nu}$ [11]. The value $\kappa_1 = 31$ (1.2) for $\mathbf{H} \perp \mathbf{c}$ ($\mathbf{H} \parallel \mathbf{c}$) will be used throughout [20], whereas ν is left as a parameter. A recent observation of the H_{c2} anisotropy suggests that ν is positive and ~ 0.01 [21].

We sketch the method to find the minimum for an arbitrary field strength [18]. Let us fix the mean flux density $\mathbf{B} \equiv (B \sin \theta \cos \varphi, B \sin \theta \sin \varphi, B \cos \theta)$ rather than the external field H , and express $\mathbf{h} = \mathbf{B} + \tilde{\mathbf{h}}$ where the spatial average of $\tilde{\mathbf{h}}$ vanishes by definition. We then transform

$$\begin{bmatrix} x \\ y \\ z \end{bmatrix} = \begin{bmatrix} \cos \theta \cos \varphi & -\sin \varphi & \sin \theta \cos \varphi \\ \cos \theta \sin \varphi & \cos \varphi & \sin \theta \sin \varphi \\ -\sin \theta & 0 & \cos \theta \end{bmatrix} \begin{bmatrix} x'/L \\ y'/L \\ z' \end{bmatrix}, \quad (2)$$

$$\boldsymbol{\eta}(\mathbf{r}) = \begin{bmatrix} \cos \frac{\phi}{2} & -\sin \frac{\phi}{2} \\ \sin \frac{\phi}{2} & \cos \frac{\phi}{2} \end{bmatrix} \begin{bmatrix} \cos \phi' & \sin \phi' \\ -i \sin \phi' & i \cos \phi' \end{bmatrix} \boldsymbol{\eta}'(\mathbf{r}'), \quad (3)$$

where ϕ , ϕ' and L are conveniently chosen as $\phi = \tan^{-1}[2\gamma \tan 2\varphi/(1-\gamma)]$, $\phi' = L^2 \cos \theta$, and $L = \{(1+\gamma-f)/[(1+\gamma-f)\cos^2 \theta + 2\kappa_5 \sin^2 \theta]\}^{1/4}$ with $f \equiv [(1-\gamma)^2 \cos^2 2\varphi + 4\gamma^2 \sin^2 2\varphi]^{1/2}$. Assuming uniformity along \mathbf{z}' direction, we then expand $\boldsymbol{\eta}'(\mathbf{r}')$ and $\tilde{\mathbf{h}}(\mathbf{r}')$ as

$$\boldsymbol{\eta}'(\mathbf{r}') = \sqrt{V} \sum_{N\mathbf{q}} \mathbf{c}_{N\mathbf{q}} \psi_{N\mathbf{q}}(\mathbf{r}'), \quad (4)$$

$$\tilde{\mathbf{h}}(\mathbf{r}') = \tilde{\mathbf{z}'} \sum_{\mathbf{K} \neq \mathbf{0}} \tilde{h}_{\mathbf{K}} \exp(i\mathbf{K} \cdot \mathbf{r}'), \quad (5)$$

where V is the system volume, $\psi_{N\mathbf{q}}$ denotes an eigenstate of the magnetic translation group in the flux density B with the Landau-level index N and the magnetic Bloch vector \mathbf{q} , and \mathbf{K} is the reciprocal lattice vector of the vortex lattice. The explicit expression of $\psi_{N\mathbf{q}}(\mathbf{r}')$ for the spacial case where one of the unit vectors of the vortex lattice, \mathbf{a}_2 , lies along the y' axis is given by

$$\psi_{N\mathbf{q}}(\mathbf{r}') = \sum_{n=-N_f/2+1}^{N_f/2} e^{i[q_{y'}(y'+0.5q_{x'})+na_{1x'}(y'+q_{x'}-0.5na_{1y'})]/l_c^2} \times \sqrt{\frac{2\pi l_c/a_2}{2^N N! \sqrt{\pi} V}} H_N\left(\frac{x'-q_{y'}-na_{1x'}}{l_c}\right) e^{-(x'-q_{y'}-na_{1x'})^2/2l_c^2}$$

with N_f^2 the number of flux quanta in the system, l_c denoting $\frac{1}{\sqrt{2}}$ of the magnetic length, and $a_{1x'}$ ($a_{1y'}$) the x' (y') component of another unit vector \mathbf{a}_1 [18]. We also consider the counterclockwise rotation of \mathbf{a}_1 and \mathbf{a}_2 around the z' axis by the angle φ'_L . Substituting Eqs. (2)-(5) into Eq. (1) and integrating over the volume, we obtain the free energy per unit volume as

$$F[\{\mathbf{c}_{N\mathbf{q}}\}, \{\tilde{h}_{\mathbf{K}}\}, B, \rho, \vartheta, \varphi'_L] = \frac{1}{V} \int f[\boldsymbol{\eta}'(\mathbf{r}'), \tilde{\mathbf{h}}(\mathbf{r}'), B] d^3 r' \quad (6)$$

where $\rho \equiv |\mathbf{a}_1|/|\mathbf{a}_2|$ and $\vartheta \equiv \cos^{-1} \frac{\mathbf{a}_1 \cdot \mathbf{a}_2}{|\mathbf{a}_1||\mathbf{a}_2|}$. This F is a desired functional which can be minimized rather easily using one of the standard minimization algorithms [22]. Due to the periodicity of the vortex lattice, we only have to perform the integration over a unit cell. The external field H is then determined through the thermodynamic relation ($H = \frac{1}{2} \frac{\partial F}{\partial B}$ in the present units). In numerical calculations we have cut the series in Eqs. (4) and (5)

at some N_c and $|\mathbf{K}_c|$, respectively, thereby obtaining a variational estimate of the free energy. The convergence can be checked by increasing N_c and $|\mathbf{K}_c|$. The choice $N_c \sim 12$ and $\mathbf{K}_c \sim$ (the third smallest) has been checked to provide correct identification of the free-energy minimum with the relative accuracy of 10^{-6} for $B/H_{c2} \gtrsim 0.1$. Though not presented here, preliminary calculations reveal that the method is also effective for $\theta \neq 0, \frac{\pi}{2}$.

The functional F has another advantage that one may enumerate possible transitions in the vortex states of multi-order-parameter systems. Much attention has been focused on this subject in connection with the observed phase diagram of superconducting UPt_3 [23]. No complete analysis has appeared yet, however, and the use of F will be quite helpful for that purpose. The features of the s -wave lattice can be summarized as follows [18]: (a) a single \mathbf{q} in Eq. (4) suffices to describe it with a choice of \mathbf{q} corresponding to the broken translational symmetry of the lattice; (b) the hexagonal (square) lattice is made up of $N=6n$ ($4n$) Landau levels (n : integer) [24,18]; (c) more general structures can be described with $N=2n$ levels, odd N 's never mixing up since those bases have finite amplitude at the core sites; (d) the expansion coefficients $\mathbf{c}_{N\mathbf{q}}$ can be chosen real for the hexagonal and square lattices. With these results on the conventional lattice, the following second-order transitions are possible in multi-component systems: (i) deformation of the hexagonal or square lattice which accompanies entry of new N 's as well as complex numbers in the expansion coefficients; (ii) mixing of another wave number \mathbf{q}_2 satisfying $\mathbf{q}_2 - \mathbf{q}_1 = \mathbf{K}/2$ [23,25]; (iii) entry of odd N 's. Though not complete, this consideration will be sufficient below.

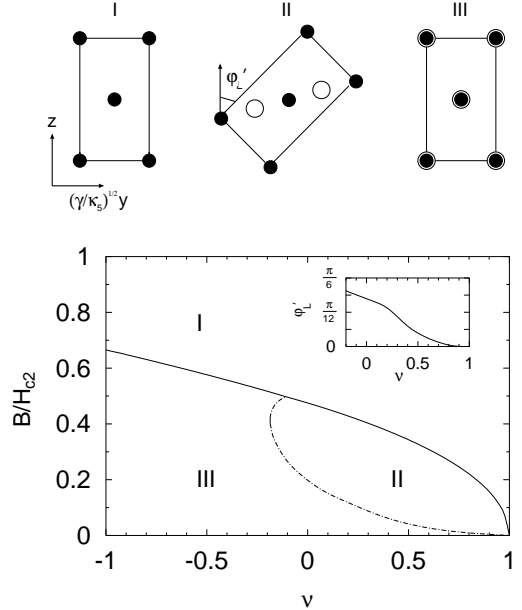


FIG. 1. Transition lines for $\mathbf{H} \parallel \mathbf{a}$ as a function of the anisotropy parameter ν . The closed (open) circles denote the zeros of η_1 (η_2). The inset plots the angle φ'_L at the I \leftrightarrow II transition as a function of ν .

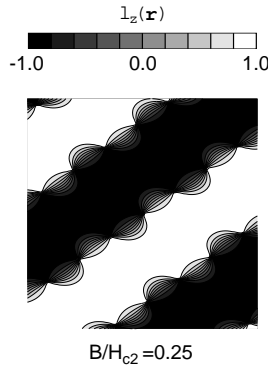


FIG. 2. Spatial variation of $l_z \equiv (\boldsymbol{\eta} \times \boldsymbol{\eta}^*) \cdot \hat{\mathbf{z}} / 2i|\eta_1||\eta_2|$ in the state II for $\nu = 0.077$ and $B/H_{c2} = 0.25$. The regions with $l_z \approx \pm 1$ correspond to the “bulk” state. See Fig. 3 for the corresponding $|\boldsymbol{\eta}(\mathbf{r})|$.

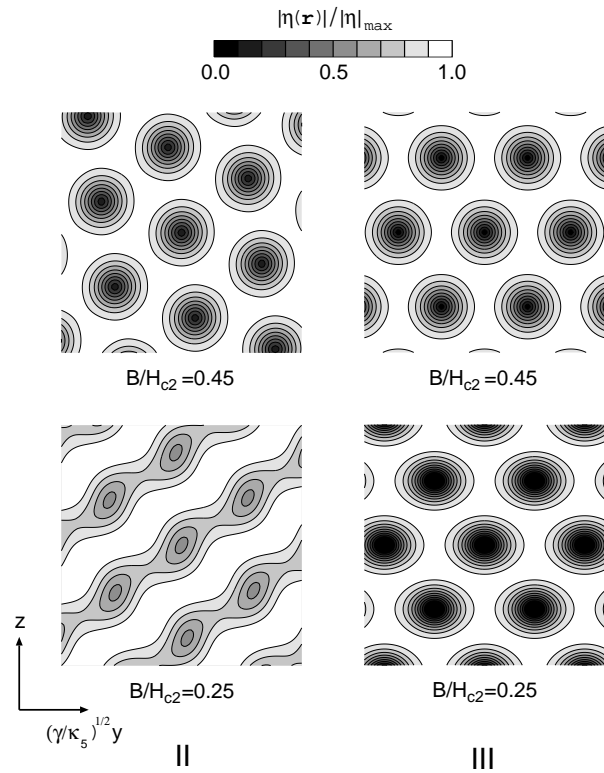


FIG. 3. A comparison of $|\boldsymbol{\eta}(\mathbf{r})|$ between the states II and III with $\nu = 0.077$ and $B/H_{c2} = 0.45, 0.25$. The amplitude $|\boldsymbol{\eta}(\mathbf{r})|$ is finite everywhere in the state II, which is brought about at the expense of the variation in l_z ; see Fig. 2.

We now present the results for $\mathbf{H} \perp \mathbf{c}$. Figure 1 shows the transition lines for $\mathbf{H} \parallel \mathbf{a}$ ($\theta = \frac{\pi}{2}; \varphi = 0$) as a function of the anisotropy parameter ν ; the one given as a function of $\gamma = \frac{1-\nu}{3+\nu}$ has qualitatively the same structure, with $\gamma = 0$ and 1 respectively corresponding to $\nu = 1$ and -1 . As already pointed out by Agterberg [11], there are three possible vortex states: the high-field region I where a hex-

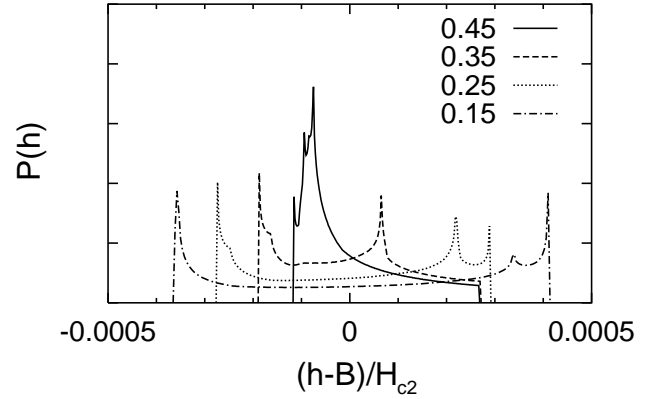


FIG. 4. The magnetic-field distribution $P(h)$ in the state II for $B/H_{c2} = 0.45, 0.35, 0.25$, and 0.15 . A characteristic double-peak structure develops as the field is decreased.

agonal lattice is stable with $\eta_2 = 0$; the region II where η_2 becomes finite with $\mathbf{q}_2 - \mathbf{q}_1$ equal to half the unit vector \mathbf{b}_1 of the reciprocal lattice, i.e. the vortex lattice is coreless with $|\boldsymbol{\eta}|$ finite everywhere; the region III where a deformed conventional lattice with $\eta_2 \neq 0$ is stable. In addition, Fig. 1 includes the following new results: (i) a full minimization with respect to $\boldsymbol{\varphi}'_L$ clarifies that the $\text{I} \leftrightarrow \text{II}$ transition is continuous as a function of ν (see the inset); (ii) high-precision calculations in the low-field region reveal that, as the field is lowered, the coreless state II is replaced via a first-order transition by the state III with cores. The reason for (ii) can be realized by looking at the variation of $l_z \equiv (\boldsymbol{\eta} \times \boldsymbol{\eta}^*) \cdot \hat{\mathbf{z}} / 2i|\eta_1||\eta_2|$ which is proportional to the magnitude of the orbital angular momentum along \mathbf{z} . As seen in Fig. 2 calculated for $\nu = 0.077$ ($\gamma = 0.3$) and $B/H_{c2} = 0.25$, one of the bulk states $l_z = \pm 1$ is alternately realized in II, and there necessarily exist lines of “defects” where l_z vanishes. Compared with III where $|\boldsymbol{\eta}|$ vanishes at points, the state II is thus energetically unfavorable at low fields. It can however be stabilized at intermediate fields by making $|\boldsymbol{\eta}|$ more uniform. Figure 3 plots $|\boldsymbol{\eta}(\mathbf{r})|$ for $\nu = 0.077$, showing how the differences between II and III develop as B/H_{c2} is decreased. In fact, only a deformation of the lattice occurs in III, whereas a layered structure also shows up in II with $|\boldsymbol{\eta}(\mathbf{r})|$ becoming more and more uniform. This rather drastic change in II can be detected by measuring the magnetic-field distribution $P(h) \equiv \frac{1}{V} \int \delta[h - h_x(\mathbf{r})] d^3r$. As seen in Fig. 4, the single peak at $B/H_{c2} = 0.45$ splits and one of them moves towards the high-field end, which originates from the development of a ridge in $h_x(\mathbf{r})$ along a valley of $|\boldsymbol{\eta}(\mathbf{r})|$. The observation of it by NMR or μ SR experiments will form a direct evidence for the state II as well as for the presence of multi-order parameters. It is also quite interesting to perform the experiments in UPt_3 where a lattice distortion has already been detected [26]. We finally point out that the second-order transition between $\text{I} \leftrightarrow \text{II}$ or $\text{I} \leftrightarrow \text{III}$ is present for an arbitrary field direction in the basal plane. A glance on the functional (1) may

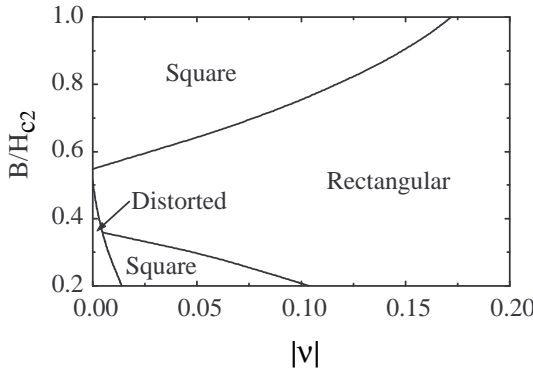


FIG. 5. The vortex-lattice phase diagram for $\mathbf{H} \parallel \mathbf{c}$ as a function of $|\nu|$ and B/H_{c2} for $\kappa_1 = 1.2$. The angle φ'_L is $\frac{\pi}{4}$ and 0 for $\nu > 0$ and $\nu < 0$, respectively.

lead to the conclusion that the transition I \leftrightarrow III disappears for a low-symmetry direction, since the term $|\eta_1|^2|\eta_2|^2$ yields those like $\eta'_1\eta'^*_2|\eta'_1|^2$. However, it does persist as the transition (i) classified in the preceding paragraph. The hexagonal lattice has been checked to be stable in the high-field region, and the phase diagram for a small $|\nu|$ is qualitatively similar to Fig. 1.

We finally present the results for $\mathbf{H} \parallel \mathbf{c}$. Figure 5 shows the vortex lattice structure as a function of $|\nu|$ and B for $\kappa_1 = 1.2$. The square lattice is stabilized near H_{c2} for small values of $|\nu|$, confirming Agterberg's result through a perturbation expansion with respect to ν ($\kappa_1 = 1.2$ corresponds Agterberg's $\kappa \sim 0.66$ for $\nu = 0$) [12]. As the field is decreased, however, the lattice deforms into a rectangular one for $|\nu| \lesssim 0.17$, followed by a further transition into the square and/or a distorted (i.e. $\rho \neq 1$; $\vartheta \neq \frac{\pi}{3}, \frac{\pi}{2}$) lattice for $|\nu| \lesssim 0.1$. The same calculation for $\kappa_1 = 2.6$ reveals that all the phase boundaries move rightward, with the distorted, square, and rectangular regions extending over $0 \leq B/H_{c2} \leq 1$ for $|\nu| \lesssim 0.004$, $0.02 \lesssim |\nu| \lesssim 0.09$, and $0.23 \lesssim |\nu|$, respectively. With κ_1 and $|\nu|$ small, the free energies of these lattices are not much different from one another, as suggested by Agterberg's ν - κ diagram near H_{c2} [12], and the present calculation reveals that there may also be field-dependent transformations among them. Although Riseman *et al.* [17] have reported an observation of the square lattice, there may exist field-dependent distortion in the diffraction pattern. A detailed experiment on the field dependence may be worth carrying out.

The author is grateful to M. Sigrist for several useful conversations, and to D. F. Agterberg for valuable comments on the original manuscript. Numerical calculations were performed on an Origin 2000 in "Hierarchical matter analyzing system" at the Division of Physics, Graduate School of Science, Hokkaido University.

- [1] Y. Maeno *et al.*, Nature **372**, 532 (1994).
- [2] T. M. Rice and M. Sigrist, J. Phys. **7**, L643 (1995).
- [3] D. F. Agterberg, T. M. Rice, and M. Sigrist, Phys. Rev. Lett. **78**, 3374 (1997).
- [4] A. P. Mackenzie *et al.*, Phys. Rev. Lett. **80**, 161 (1998).
- [5] K. Ishida *et al.*, Phys. Rev. B **56**, R505 (1997).
- [6] K. Ishida *et al.*, Nature **396**, 658 (1998).
- [7] R. Jin *et al.*, Phys. Rev. B **59**, 4433 (1999).
- [8] C. Honerkamp and M. Sigrist, Prog. Theor. Phys. **100**, 53 (1998).
- [9] M. Yamashiro, Y. Tanaka, and S. Kashiwaya, J. Phys. Soc. Jpn. **67**, 3364 (1998).
- [10] G. M. Luke *et al.*, Nature **394**, 558 (1998).
- [11] D. F. Agterberg, Phys. Rev. Lett. **80**, 5184 (1998).
- [12] D. F. Agterberg, Phys. Rev. B **58**, 14484 (1998).
- [13] R. Heeb and D. F. Agterberg, Phys. Rev. B **59**, 7076 (1999).
- [14] A. A. Abrikosov, Zh. Eksp. Teor. Fiz. **32**, 1442 (1957) [Sov. Phys. JETP **5**, 1174 (1957)].
- [15] G. Bruls *et al.*, Phys. Rev. Lett. **65**, 2294 (1990).
- [16] S. Adenwalla *et al.*, Phys. Rev. Lett. **65**, 2298 (1990).
- [17] T. M. Riseman *et al.*, Nature **396**, 242 (1998).
- [18] T. Kita, J. Phys. Soc. Jpn. **67**, 2067 (1998).
- [19] K. Machida, T. Fujita, and T. Ohmi, J. Phys. Soc. Jpn. **62**, 680 (1993).
- [20] K. Yoshida *et al.*, J. Phys. Soc. Jpn. **65**, 2220 (1996).
- [21] Z. Q. Mao, T. Akima, T. Ando, and Y. Maeno, unpublished.
- [22] See, e.g. W. H. Press, S. A. Teukolsky, W. T. Vetterling and B. P. Flannery: *Numerical Recipes in C* (Cambridge University Press, Cambridge, 1988) Chap. 10.
- [23] See, e.g. M. Sigrist and K. Ueda, Rev. Mod. Phys. **63**, 239 (1991); J. A. Sauls, Adv. Phys. **43**, 1313 (1994); I. A. Luk'yanchuk and M. E. Zhitomirsky, Supercond. Rev. **1**, 207 (1995).
- [24] J. C. Ryan and A. K. Rajagopal: Phys. Rev. B **47**, 8843 (1993).
- [25] A. Garg and D.-C. Chen, Phys. Rev. B **49**, 479 (1994).
- [26] U. Yaron *et al.*, Phys. Rev. Lett. **78**, 3185 (1997).